ISSN 1063-7834, Physics of the Solid State, 2007, Vol. 49, No. 5, pp. 918–924. © Pleiades Publishing, Ltd., 2007.
Original Russian Text © V.S. Zakhvalinskiĭ, R. Laiho, K.G. Lisunov, E. Lähderanta, P.A. Petrenko, Yu.P. Stepanov, V.N. Stamov, M.L. Shubnikov, A.V. Khokhulin, 2007, published in Fizika Tverdogo Tela, 2007, Vol. 49, No. 5, pp. 870–876.

MAGNETISM AND FERROELECTRICITY

Variable-Range Hopping Conduction in $LaMnO_{3+\delta}$

V. S. Zakhvalinskiĭ[a], R. Laiho[b], K. G. Lisunov[c], E. Lähderanta[d], P. A. Petrenko[c], Yu. P. Stepanov[e], V. N. Stamov[c], M. L. Shubnikov[e], and A. V. Khokhulin[a]

[a] *Belgorod State University, Belgorod, 308015 Russia*
[b] *Wihuri Physical Laboratory, University of Turku, Turku, FIN-20014 Finland*
[c] *Institute of Applied Physics, Academy of Sciences of Moldova, Academiei 5, Chisinau, MD-2028 Moldova*
[d] *Department of Physics, Lappeenranta University of Technology, Lappeenranta, FIN-53851 Finland*
[e] *Ioffe Physicotechnical Institute, Russian Academy of Sciences, Politekhnicheskaya ul. 26, St. Petersburg, 194021 Russia*
e-mail: yustepanov.solid@mail.ioffe.ru

Received July 18, 2006; in final form, September 18, 2006

Abstract—The temperature dependence of the electrical resistivity $\rho(T)$ for ceramic samples of $LaMnO_{3+\delta}$ ($\delta = 0.100$–0.154) are studied in the temperature range $T = 15$–350 K, in magnetic fields of 0–10 T, and under hydrostatic pressures P of up to 11 kbar. It is shown that, above the ferromagnet–paramagnet transition temperature of $LaMnO_{3+\delta}$, the dependence $\rho(T)$ of this compound obeys the Shklovskii–Efros variable-range hopping conduction: $\rho(T) = \rho_0(T)\exp[(T_0/T)^{1/2}]$, where $\rho_0(T) = AT^{9/2}$ (A is a constant). The density of localized states $g(\varepsilon)$ near the Fermi level is found to have a Coulomb gap Δ and a rigid gap $\gamma(T)$. The Coulomb gap Δ assumes values of 0.43, 0.46, and 0.48 eV, and the rigid gap satisfies the relationship $\gamma(T) \approx \gamma(T_v)(T/T_v)^{1/2}$, where T_v is the temperature of the onset of variable-range hopping conduction and $\gamma(T_v) = 0.13$, 0.16, and 0.17 eV for $\delta = 0.100$, 0.125, and 0.154, respectively. The carrier localization lengths $a = 1.7$, 1.4, and 1.2 Å are determined for the same values of δ. The effect of hydrostatic pressure on the variable-range hopping conduction in $LaMnO_{3+\delta}$ with $\delta = 0.154$ is analyzed, and the dependences $\Delta(P)$ and $\gamma_v(P)$ are obtained.

PACS numbers: 75.47.Lx, 74.25.Fy, 74.62.Dh, 75.47.Gk, 75.30.Et

DOI: 10.1134/S1063783407050198

1. INTRODUCTION

The compound $LaMnO_{3+\delta}$ belongs to hole-doped mixed-valence (Mn^{3+}–Mn^{4+}) perovskite manganites exhibiting colossal magnetoresistance [1]. The magnetic phase diagram of these compounds includes the high-temperature paramagnetic, ferromagnetic, and spin glass regions [1, 2].

The hole doping of $LaMnO_{3+\delta}$ differs from that used for close analogs of this compound, for instance, $La_{1-x}Ca_xMnO_3$. In the latter materials, holes are created by substituting Ca^{2+} ions for La^{3+} ions in the lattice. Because excess oxygen cannot occupy interstitial sites in the perovskite structure [3, 4], the nonstoichiometry of $LaMnO_{3+\delta}$ can be associated with the formation of cation vacancies. The concentration of cation vacancies $\delta' = (2/3)\delta$ corresponds to the relative hole concentration (or the Mn^{4+}/Mn^{3+} ratio) $c = 2\delta$. The absence of Ca ions leads to a decrease in the degree of disorder in the lattice and to a more uniform hole distribution in $LaMnO_{3+\delta}$ as compared to that in $La_{1-x}Ca_xMnO_3$ [5].

In compounds exhibiting colossal magnetoresistance, one observes hopping conduction of small-radius polarons (associated with local Jahn–Teller lattice distortions) over nearest neighbors above room temperature, which obeys an Arrhenius-type equation [1]. Below room temperature, hopping conduction depends strongly on the specific features in the density of localized states $g(\varepsilon)$ near the Fermi level μ [6]. Scanning tunneling spectroscopy of $La_{0.8}Ca_{0.2}MnO_3$ films revealed a complex structure of the density of localized states near the Fermi level μ, which includes the range characterized by a quadratic dependence $g(\varepsilon)$ with a width $\Delta \sim 0.5$ eV (soft gap) and the range with $g(\varepsilon) = 0$ and $\gamma(T) \sim 0.11$ eV (rigid gap) [7]. The soft gap was explained by the effect of Coulomb interaction of charge carriers (the Coulomb gap [8]), whereas the rigid gap was attributed to the Jahn–Teller effect [7].

As the temperature decreases, it becomes increasingly more favorable energywise for carriers to hop beyond the region of nearest sites, thus giving rise to variable-range hopping conduction [8, 9]. The Mott conduction occurs under the conditions where the density of localized states near the Fermi level μ is constant and finite [9]. The existence of a Coulomb gap brings about another kind of deviation from the Arrhenius law, namely, the Shklovskii–Efros (SE) variable-range hopping conduction [8]. Moreover, the rigid gap also affects the variable-range hopping conduction [6]. A

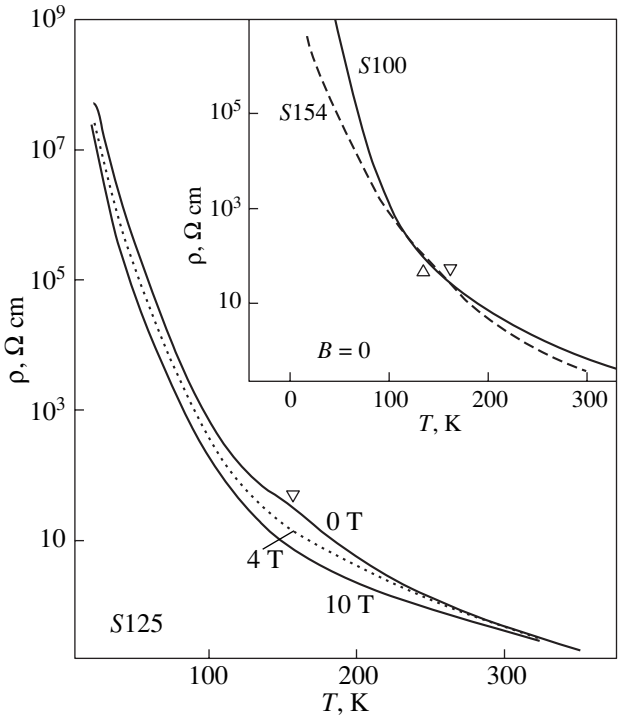

Fig. 1. Temperature dependences of the electrical resistivity measured for the $LaMnO_{3+\delta}$ sample (*S*125) in magnetic fields $B = 0$, 4, and 10 T and for samples *S*100 and *S*154 in a zero field (inset).

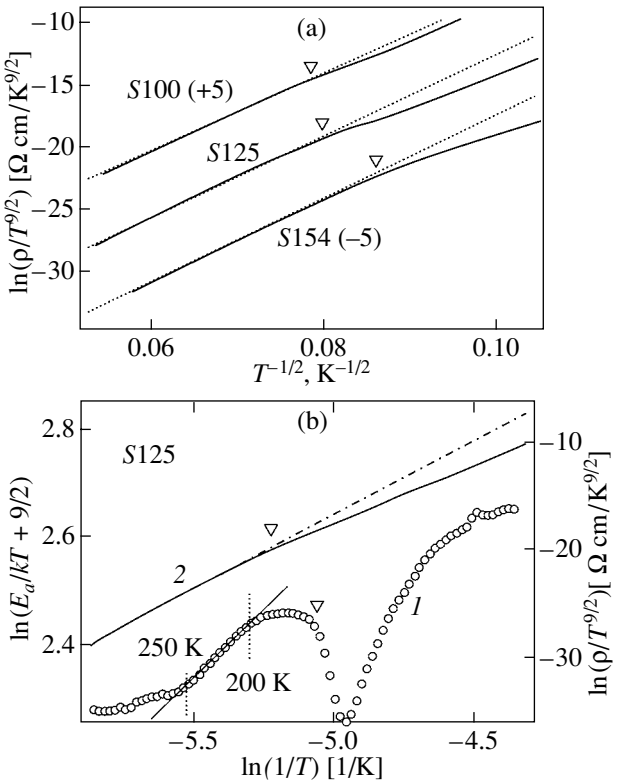

Fig. 2. (a) Dependences of $\ln(\rho/T^{9/2})$ on $T^{-1/2}$ for $LaMnO_{3+\delta}$ samples (*S*100, *S*125, and *S*154). Two curves are shifted along the *y* axis by ±5 units. (b) Dependences of (*1*) $\ln(E_a/kT + 9/2)$ on $\ln(1/T)$ and (*2*) $\ln(\rho/T^{9/2})$ on $T^{-1/2}$ for the $LaMnO_{3+\delta}$ sample (*S*125).

comprehensive analysis of the electrical resistivity [6] and thermopower [10] in $La_{0.7}Ca_{0.3}Mn_{1-y}Fe_yO_3$ above the Curie temperature T_C led to $\Delta \approx 0.4$ eV and $\gamma(T) \approx \gamma(T_v)(T/T_v)^{1/2}$, where $\gamma(T_v) = 0.16$–0.12 eV decreases with increasing *y* and assumes values close to those obtained in [7].

In this work, we studied the electrical conductivity and magnetoresistance of $LaMnO_{3+\delta}$ samples with the aim of obtaining information regarding the conduction mechanisms and the carrier energy spectrum, including data on the structure of the density of localized states near the Fermi level.

2. PREPARATION OF SAMPLES AND THEIR CHARACTERIZATION

Ceramic samples of $LaMnO_{3+\delta}$ with $\delta = 0.100$, 0.125, and 0.154 (referred to as *S*100, *S*125, and *S*154, respectively) were prepared by standard solid-phase technology. The specific features of this technology and subsequent annealing in Ar, O_2, and air were described in considerable detail in [5]. X-ray powder diffraction analysis revealed that sample *S*100 has a cubic structure (space group *Pm*3*m*) with small rhombohedral distortions, whereas samples *S*125 and *S*154 have a rhombohedral structure (space group *R*-3*c*). The parameter δ, which is related to the La and Mn vacancy concentration δ' and determines the hole concentration *c*, was determined by iodometric titration [5].

3. RESULTS AND DISCUSSION

3.1. Temperature Dependence of the Electrical Resistivity

The electrical resistivity was studied by the four-point probe technique in the transverse magnetic field configuration in the range of magnetic fields $B = 0$–10 T. The samples were contained in a helium gas-exchange Dewar, where their temperature could be varied in the range 4.2–350 K with an accuracy of 0.5%. The temperature dependences of the electrical resistivity of samples *S*100, *S*125, and *S*154 are shown in Fig. 1 (with magnetic fields applied to one of the samples). Open triangles in Figs. 1 and 2 identify the paramagnetic–ferromagnetic phase transition temperatures T_C.

3.2. Analysis and Discussion of the Dependences ρ(T)

The electrical resistivity of $LaMnO_{3+\delta}$ above T_C was analyzed by fitting it with a universal relationship,

$$\rho(T) = \rho_0(T)\exp[(T_0/T)^p], \quad (1)$$

where T_0 is the characteristic temperature; and $p = 1$ for conduction over the nearest sites (in this case, T_0 is usually replaced by the activation energy $E_0 \equiv kT_0$), $p = 1/4$ for the Mott-type variable-range hopping conduction [9], and $p = 1/2$ for the Shklovskii–Efros variable-range hopping conduction [8]. If the condition $\Gamma \equiv [kT(T_0/T)^p a/(2\hbar s)]^2 \gg 1$ is met, the preexponential factor in Eq. (1) can be written in the form

$$\rho_0(T) = AT^m. \quad (2)$$

Here,

$$A = Ca^{11}T_0^{(7+q)p}, \quad (3)$$

a is the carrier localization length, s is the velocity of sound, and C is a constant [6]. For the Shklovskii–Efros variable-range hopping conduction, we have $m = 9/2$ or 5/2, while for the Mott variable-range hopping conduction, $m = 25/4$ or 21/4, if the localized-carrier wave function has the form $\psi_1(r) \sim \exp(-r/a)$ for $q = 0$ or $\psi_2(r) \sim r^{-1}\exp(-r/a)$ for $q = 4$ in Eq. (3), respectively. The wave function ψ_2 is used in the case where the fluctuating short-range potential associated with lattice disorder strongly affects the carrier localization [8]. For (adiabatic) conduction over the nearest centers, we have $m = 1$ for any values of ψ, q, and Γ [9]. In Eq. (1), $T_0 = T_{0M}$ or T_{0SE} for $p = 1/4$ or 1/2, respectively, where

$$T_{0M} = \beta_M/[kg(\mu)a^3], \quad T_{0SE} = \beta_{SE}e^2/(\kappa ka), \quad (4)$$

κ is the dielectric constant, $\beta_M = 21$, and $\beta_{SE} = 2.8$ [8]. If the rigid gap is present, i.e., $\gamma < \Delta$, the variable-range hopping conduction satisfies Eq. (1) with $p = 1/2$, in which T_0 [6] is given by the relationship

$$T_0 = \left(\frac{\gamma}{2k\sqrt{T}} + \sqrt{\frac{\gamma^2}{4k^2T} + T_{0SE}}\right)^2. \quad (5)$$

As can be seen from Eq. (4), T_{0SE} and T_{0M} do not depend on T for constant a or $g(\mu)a^3$, respectively. As follows from Eq. (5), T_0 does not depend on T if, in addition, one of the following conditions is met: (1) $\gamma/(2kT) \ll (T_{0SE}/T)^{1/2}$ and $\gamma \sim T$ or (2) $\gamma \sim T^{1/2}$. For case 1, we have $T_0 = T_{0SE}$ because $(T_0/T)^{1/2} \approx (T_{0SE}/T)^{1/2} + \gamma/(2kT)$ and, if $\gamma \sim T$, the second term does not depend on T and can be included in the preexponential factor, whereas the relationship $T_0 \neq T_{0SE}$ holds for case 2.

Equation (1) allows a better fit to the temperature dependences of the electrical resistivity for constant T_0 if we set $p = 1/2$ and $m = 9/2$ in the range limited by a temperature close to T_C (Fig. 2a). The fact that $\rho(T)$ of the samples studied is consistent with the Shklovskii–Efros variable-range hopping conduction mechanism, which satisfies the $\Gamma \gg 1$ and $\psi = \psi_1$ conditions for the above values of p and m, is borne out by an analysis of the local activation energy $E_a(T) \equiv \delta\ln\rho(T)/d(kT)^{-1}$ [8]. As can be seen from Eq. (1), if T_0 does not depend on T, the dependence $E_a(T)$ can be written in the form $\ln[E_a/(kT) + m] = \ln p + p\ln T_0 + p\ln(1/T)$. Figure 2b suggests that the dependence of $\ln[E_a/kT + 9/2]$ on $\ln(1/T)$ is linear in the same temperature range as in Fig. 2a, with the slope corresponding to $p = 1/2$. The linear parts of the graphs in Fig. 2 were used to find the values $T_0 = 9.8 \times 10^4$, 10.8×10^4, and 11.3×10^4 K and the temperatures of the onset of the variable-range hopping conduction $T_v = 250$, 250, and 270 K for samples *S*100, *S*125, and *S*154, respectively. By substituting these parameters into the equation [6]

$$\Delta \approx k(T_0T_v)^{1/2}, \quad (6)$$

we obtained the following values of the Coulomb gap: $\Delta = 0.43$, 0.46, and 0.48 eV for the same samples.

The existence of a temperature range within which T_0 is constant (Fig. 2) implies that we are considering one of the cases commented on when we discussed Eq. (5). To pinpoint this case, we studied the temperature dependence of the electrical resistivity in a magnetic field. The localization length of small-radius polarons in the paramagnetic phase varies in a field as $a(B) = a(0)(1 + b_1B^2)$, where $b_1 \sim \chi(T)$ [11]. As follows from Eqs. (4)–(6), for $b_1B^2 \ll 1$, we have $T_0(B) = T_0(0)(1 - b_2B^2)$, where $b_2 = b_1T_{0SE}(0)\{T_0(0) - [T_0(0)/T]^{1/2}\gamma/(2k)\}^{-1}$, provided γ does not depend on B. Hence, we arrive at the relationship

$$\gamma(T) = 2[(b_1/b_2 - 1)/(2b_1/b_2 - 1)]k[T_0(0)T]^{1/2}. \quad (7)$$

Close to $T_v \gg T_C$, the magnetic susceptibility χ varies very little with temperature [5]. Hence, the dependences of T_0 and A on B in the temperature range near T_v can be derived from a linear approximation of the $\ln(\rho/T^{9/2})$ versus $T^{-1/2}$ graphs obtained in a magnetic field. The $a(B)/a(0)$ ratio can be found from Eq. (3). It was established that the dependences of $a(B)/a(0)$ on B^2 and $T_0(B)/T_0(0)$ on B^2 are linear functions up to $B = 10$ T for samples *S*100 and *S*125 and almost up to 8 T for sample *S*154 (these dependences are illustrated for sample *S*125 in Fig. 3). The ratios $b_1/b_2 = 1.24 \pm 0.04$, 1.26 ± 0.06, and 1.28 ± 0.05 for samples *S*100, *S*125, and *S*154, respectively, are above unity and outside the error limits. According to Eq. (7), this implies the existence of a nonzero rigid gap that depends on T as

$$\gamma(T) \approx \gamma(T_v)(T/T_v)^{1/2}, \quad (8)$$

where $\gamma(T_v) = 0.13$, 0.16, and 0.17 eV for samples *S*100, *S*125, and *S*154, respectively.

The carrier localization length was found using the expression for the density of localized states outside the Coulomb gap: $g_0 \approx N_0\phi\sigma\eta/W$ [12], where $N_0 = 1.74 \times 10^{22}$ cm^{-3} is the Mn site concentration, W is the width of the localized-state band, $\eta \approx c$, $\phi \approx 0.5$ is the geometric factor, and $\sigma \approx 1 - c$ [12]. The values of W were calculated from the expression $kT_C \approx 0.05Wc(1 - c)$ [11],

where the temperatures T_C were derived from magnetization measurements [5]. Next, the relationship $g_0 = (3/\pi)(\kappa^3/e^6)[\Delta - \gamma(T_v)]^2$ [6] was used to obtain $\kappa \approx 3.5$. The values a = 1.7, 1.4, and 1.2 Å were found from Eqs. (4) and (6). The values of a and T_0 obtained by us here show directly that the condition $\Gamma \gg 1$ is met for all the $LaMnO_{3+\delta}$ samples studied.

The value $\kappa \approx 3.5$ is close to the values found earlier for $La_{1-x}Ba_xMnO_3$ [13], $La_{0.7}Ca_{0.3}Mn_{1-y}Fe_yO_3$ [6], and $LaMnO_{3+\delta}$ [14]. The values of κ in these cases are substantially smaller than the static dielectric constant κ_0 = 16 [15]. On the other hand, κ is much closer to κ_p than to κ_0, whereas we have $\kappa = \kappa_0$ for doped semiconductors [16]. The point is that, in the perovskite manganites, the concentration of carriers (which is equal to that of holes) is much higher than that in doped semiconductors. Moreover, carriers in the perovskite manganites are polarons of small radius and, in nonmagnetic semiconductors, the contribution from polarons of small radius is very small [8]. As a result of the high concentration of polarons, their average separation is comparable to the lattice parameters. On the other hand, the major contribution to Δ comes from interaction among the nearest carriers. The space around a polaron is characterized, however, not by the parameter κ_0 but by the quantity $\kappa_p = (\kappa_\infty^{-1} - \kappa_0^{-1})^{-1}$, where κ_∞ is the high-frequency permittivity [9, 17]. The electrostatic interaction between polarons at a distance R does not obey the conventional Coulomb relationship and can be written in the form $U \approx e^2/(\kappa_p R)$, i.e., assuming $\kappa \approx \kappa_p$. The Coulomb gap widths Δ in $LaMnO_{3+\delta}$ obtained by us are close to those found for $La_{0.8}Ca_{0.2}MnO_3$ [7] and $La_{0.7}Ca_{0.3}Mn_{1-y}Fe_yO_3$ [6].

The values of a are consistent with the assumption that small-radius polarons are formed in perovskite manganites [9]. Moreover, a decreases with increasing δ, as should be expected in accordance with the increase in the degree of localization with increasing perovskite structure distortions. The values of $\gamma(T_v)$ are similar to those obtained for $La_{0.8}Ca_{0.2}MnO_3$ [7] and $La_{0.7}Ca_{0.3}Mn_{1-y}Fe_yO_3$ [6]. On the other hand, they are comparable to the activation energy of adiabatic hopping of small-radius polarons over nearest neighbors, $E_0 \approx E_b/2$, where E_b is the polaron binding energy [1]. Hence, the origin of the rigid gap in the perovskite manganites can be associated with the polaron nature of the carriers. In performing a hop, the electron has to annihilate polarization in the initial position and create it in the final position. It is the existence of a minimum energy required for a hop to be realized that gives rise to a rigid gap in the density of localized states near the Fermi level μ, provided local lattice distortions account primarily for carrier localization. It is the case of reduced lattice disorder [5] and of lattice distortions increasing with increasing δ that is realized in $LaMnO_{3+\delta}$, and this can account primarily for the increase in γ with increasing δ.

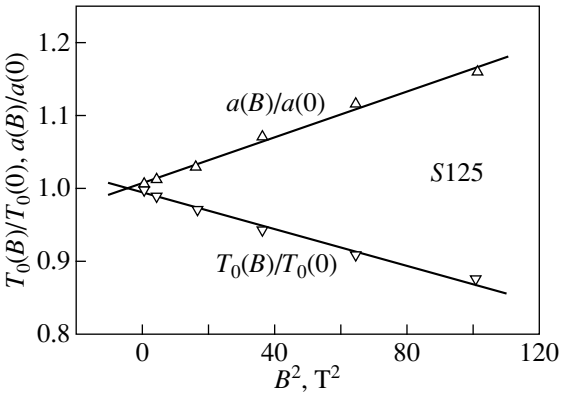

Fig. 3. Dependences of $a(B)/a(0)$ and $T_0(B)/T_0(0)$ on B^2 for the $LaMnO_{3+\delta}$ sample (*S*125).

3.3. Study of the Electrical Resistivity under Pressure

The measurements of the dependences $\rho(T)$ were performed by the four-point probe technique under hydrostatic pressures of up to 11 kbar. The pressure was generated in a Be–Cu cell with a gasolene–oil mixture serving as a pressure-transmitting liquid.

As can be seen from Fig. 4a, the electrical resistivity of sample *S*154 exhibits activation behavior. The $\rho(T)$ curve has slight bends near T_C, which are identified for P = 1 bar and 11 kbar by open triangles. The value T_C(1 bar) = 129 K is close to $T_C = 135 \pm 1$ K, which is derived from magnetization measurements in the absence of excess pressure [5]. The dependence $T_C(P)$ shown in Fig. 5 is nearly linear with $dT_C/dP = 1.6 \pm 0.2$ K/kbar, $d\ln T_C/dP = 0.012 \pm 0.002$ kbar^{-1}, and a maximum change of ~14% (at 11 kbar). This dependence $T_C(P)$ and the values of dT_C/dP are typical of perovskite manganites [18, 19]. As can be seen from Fig. 4a, $\rho(T)$ decreases with increasing P for all temperatures.

As was already shown before, in $LaMnO_{3+\delta}$ at atmospheric pressure and for $T > T_C$, the dependence $\rho(T)$ follows the Shklovskii–Efros variable-range hopping conduction law (Eq. (1) for p = 1/2, m = 9/2, and $A \sim T_0^{7/2}$). Expression (5) for the characteristic temperature T_0 can be recast for $\gamma_v \equiv \gamma(T_v)$ in the form

$$T_0 = \left(\frac{\gamma_v}{2k\sqrt{T_v}} + \sqrt{\frac{\gamma_v^2}{4k^2 T_v} + T_{0SE}}\right)^2. \qquad (9)$$

The quantities Δ and γ_v are related to T_0 and T_v and the density of localized states g_0 outside the Coulomb

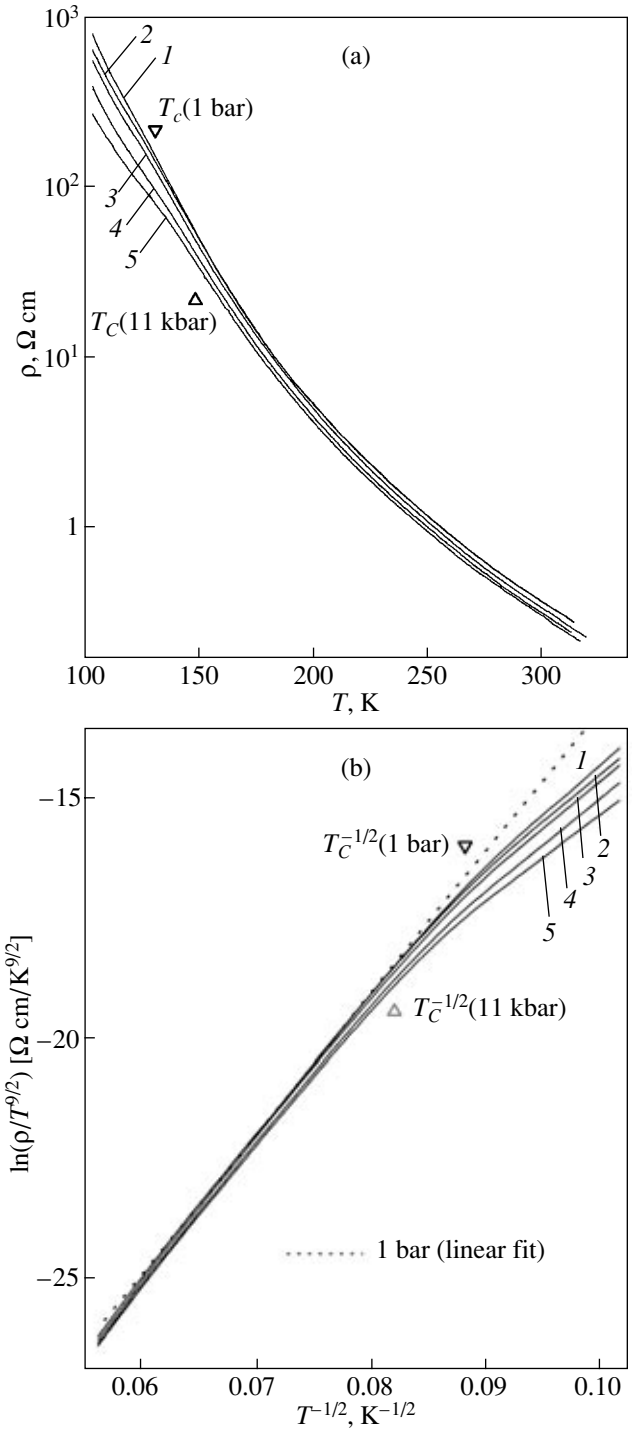

Fig. 4. Dependences of (a) ρ on T and (b) $\ln(\rho/T^{9/2})$ on $T^{-1/2}$ at different pressures P = (*1*) 0.001, (*2*) 5, (*3*) 7, (*4*) 9, and (*5*) 11 kbar.

gap through Eq. (6) and the expression [6]

$$g_0 \approx (3/\pi)(\kappa^3/e^6)(\Delta - \gamma_v)^2. \qquad (10)$$

As can be seen from Fig. 4b, the dependence of $\ln[\rho(T)/T^{9/2}]$ on $T^{-1/2}$ obtained under pressure contains

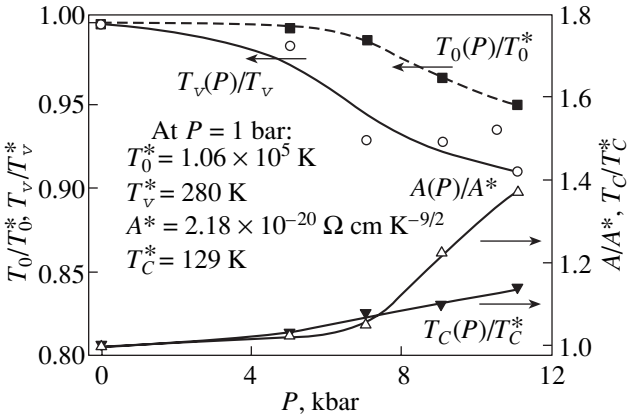

Fig. 5. Dependences of T_C/T_C^*, T_0/T_0^*, T_v/T_v^*, and A/A^* on the pressure. The solid and dashed lines are drawn to aid the eye.

a linear portion below T_v. Deviations from linearity are observed for $T \longrightarrow T_C$ (the values of $T_C^{-1/2}$ are identified by open triangles for P = 1 bar and 11 kbar). These dependences were used to derive the values of $T_v(P)$, $T_0(P)$, and $A(P)$ presented in Fig. 5. The values of $\Delta(P)$ derived from Eq. (6) are given in Fig. 6a. The relative variation in the localization length $a(P)/a^*$ (all symbols with an asterisk refer to P = 1 kbar) was obtained using Eq. (3) and is shown in Fig. 6b.

The macroscopic (T_0, T_v, and A) and microscopic (Δ, γ_v, g_0, and a) parameters are interrelated. This interrelation is given by Eqs. (3)–(10). Therefore, we present below a quantitative analysis of the dependence $\Delta(P)$ only. Equation (8) can be used to obtain

$$\Delta(P) \approx \gamma_v(P) + (\pi/3)^{1/2} e^3 g_0^{1/2}(P)/(\kappa^{3/2}); \qquad (11)$$

and from Eq. (7), we have

$$\gamma_v(P) = k[T_v(P)/T_0(P)]^{1/2} \times \{T_0(P) - \beta e^2/[\kappa k a^* a(P)/a^*]\}. \qquad (12)$$

On the other hand, $g_0(P) = \varphi\sigma\eta N(P)/W(P)$ [12], where $\varphi \approx 0.5$, $\sigma = 1 - c$, and $\eta = c$ are numerical parameters which are constant for $c = 2\delta = 0.308$ (see above); $N(P) = N^*(1 + 3P/G)$; $N^* \approx 1.7 \times 10^{22}$ cm^{-3} is the Mn concentration in $LaMnO_{3+\delta}$ at P = 1 bar; $G = 5 \times 10^{11}$ N/m^2 is Young's modulus [20]; and $W(P) \approx 20kT_C(P)/[c(1 - c)]$ is the localized-carrier band width [11]. Hence, the dependence $\Delta(P)$ can be found from Eqs. (6)–(9) using the dependences $T_0(P)$, $T_v(P)$, and $T_C(P)$ in Fig. 5a and $a(P)/a^*$ in Fig. 6 and two fitting parameters (a^* and κ). The dependence $\Delta(P)$ thus calculated is shown in Fig. 6a. The best fit of the $\Delta(P)$ function to experimental data is reached for $a^* \approx 1.7$ Å and $\kappa \approx 3.75$; these values are consistent with the values $a^* \approx 1.2$–1.7 Å and $\kappa \approx 3.5$ obtained for $LaMnO_{3+\delta}$ (see

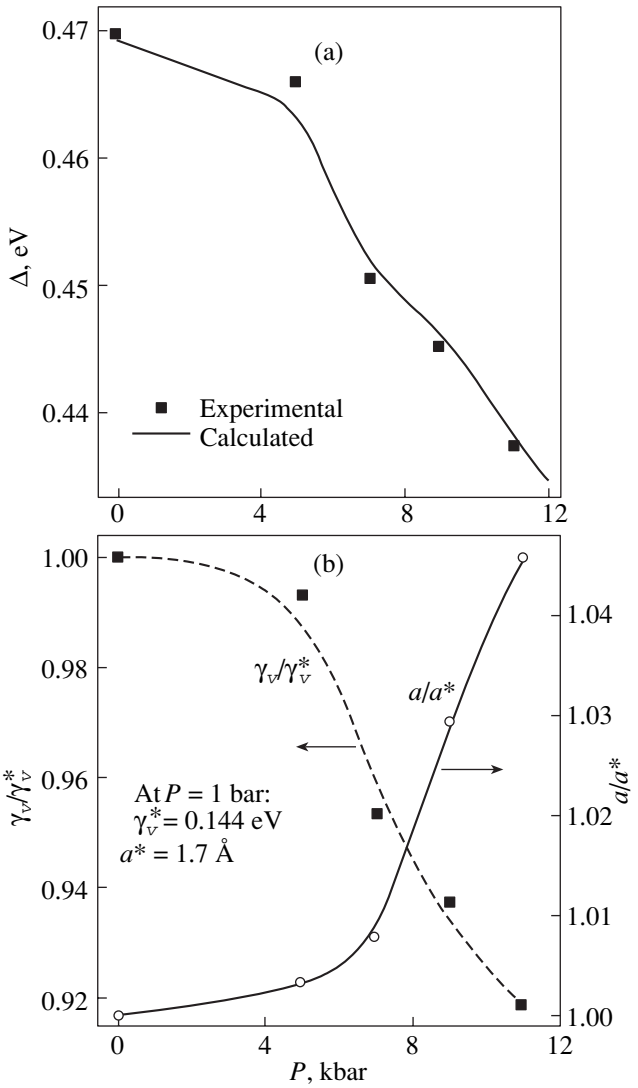

Fig. 6. Dependences of (a) the Coulomb gap Δ and (b) the ratios γ_v/γ_v^* and a/a^* on the pressure. The solid and dashed lines in panel (b) are drawn to aid the eye.

Section 3.2) in a different way, i.e., from magnetization measurements performed with no pressure applied. The method described above was also employed to calculate $\gamma_v^* \approx 0.144$ eV (cf. $\gamma_v \approx 0.13$–0.17 eV, the values derived above from Eq. (8)) and the $\gamma_v(P)$ function plotted in Fig. 6b.

Because $T_C(P) \sim W(P)$, the observed effect of pressure on T_C should be assigned to the increasing width of the localized-carrier band. On the other hand, it is known that the pressure-induced variation in W in perovskite manganites is actually driven by two factors, namely, (1) spatial effects or an increase in the Mn–O–Mn bond angles and a decrease in the corresponding bond lengths, which increases the electron transfer integral and enhances double exchange interaction; and (2) the polaron nature of carriers associated with the effect of pressure on the electron–phonon coupling and the corresponding Jahn–Teller distortions [18, 19]. In addition, in accordance with the assumed origin of the rigid gap (see Section 3.2), we can write $\gamma_v = E_p/2 - E_d/2$, where E_p is the depth of the polaron potential well associated with the polarization of the medium and E_d is the width of the electron potential energy distribution governed by disorder. Because the degree of disorder in $LaMnO_{3+\delta}$ is small [5], the observed decrease in γ_v with pressure should be connected primarily with suppression of the polaron effect by a pressure that decreases E_p. The decrease in E_p implies a decrease in the degree of localization, which brings about an increase in $a(P)$, as is seen in Fig. 6b. On the other hand, the effect of pressure on γ_v is weaker (up to ~8%) than that on T_C (up to ~14%), which can be explained by the absence of an effect of factor 1 on $\gamma_v(P)$ or by this effect being smaller than that on $T_C(P)$.

4. CONCLUSIONS

Thus, we studied the temperature dependences of the electrical conductivity and magnetoresistance of ceramic $LaMnO_{3+\delta}$ samples (δ = 0.100, 0.125, and 0.154). An analysis of these dependences suggests that the behavior of the resistivity of $LaMnO_{3+\delta}$ in the paramagnetic phase in the temperature range between T_C and T_v, which is ~250–270 K, is governed by the complex structure of the density of localized states near the Fermi level. We established the presence of a soft Coulomb gap Δ and a rigid gap γ, whose widths increase with increasing δ. The increase in the gap width δ is accounted for by the increasing hole concentration $c = 2\delta$ and the corresponding enhancement of the carrier Coulomb interaction. The existence of the rigid gap γ should possibly be attributed to the formation of small-radius polarons, and its increase with increasing δ, to the enhancement of lattice distortions under conditions of reduced disorder. The observed dependence of the localization length a on δ is accounted for by the increasing hole localization as a result of increasing lattice distortions.

The pressure dependences of the macroscopic parameters $\Delta(P)$, $\gamma_v(P)$, and $a(P)$ obtained in the studies of the effect of hydrostatic pressure on the variable-range hopping conduction in $LaMnO_{3+\delta}$ can be explained by the increase in the electron band width and the decrease in the polaron effect with increasing pressure.

ACKNOWLEDGMENTS

This study was supported by the Wihuri Physical Laboratory, University of Turku (Finland), and the International Association of Assistance for the Promotion of Cooperation with Scientists from the New Independent States of the Former Soviet Union, project INTAS no. 00-728.

REFERENCES

1. J. M. D. Coey, M. Viret, and S. von Molnar, Adv. Phys. **48**, 167 (1999).
2. R. Laiho, E. Lähderanta, J. Salminen, K. G. Lisunov, and V. S. Zakhvalinskii, Phys. Rev. B: Condens. Matter **63**, 094405 (2001).
3. J. Töpfer and J. B. Goodenough, J. Solid State Chem. **130**, 117 (1997).
4. B. Dabrowski, X. Xoing, Z. Bukowski, R. Dybzinski, P. W. Klamut, J. E. Siewenie, O. Chmaissem, J. Shaffer, C. W. Kimball, J. D. Jorgesen, and S. Short, Phys. Rev. B: Condens. Matter **60**, 7006 (1999).
5. R. Laiho, K. G. Lisunov, E. Lähderanta, P. A. Petrenko, J. Salminen, V. N. Stamov, Yu. P. Stepanov, and V. S. Zakhvalinskii, J. Phys. Chem. Solids **64**, 2313 (2003).
6. R. Laiho, K. G. Lisunov, E. Lähderanta, P. A. Petrenko, J. Salminen, M. A. Shakhov, M. O. Safontchik, V. N. Stamov, M. L. Shubnikov, and V. S. Zakhvalinskii, J. Phys.: Condens. Matter **14**, 8043 (2002).
7. A. Biswas, S. Elizabeth, A. K. Raychaudhuri, and H. L. Bhat, Phys. Rev. B: Condens. Matter **59**, 5368 (1999).
8. B. I. Shklovskii and A. L. Efros, *Electronic Properties of Doped Semiconductors* (Springer, Berlin, 1984).
9. N. F. Mott and E. A. Davies, *Electron Processes in Non-Crystalline Materials* (Clarendon, Oxford, 1979).
10. R. Laiho, K. G. Lisunov, E. Lähderanta, V. N. Stamov, V. S. Zakhvalinskii, A. I. Kurbakov, and A. E. Sokolov, J. Phys.: Condens. Matter **16**, 881 (2004).
11. C. M. Varma, Phys. Rev. B: Condens. Matter **54**, 7328 (1996).
12. M. Viret, L. Ranno, and J. M. D. Coey, Phys. Rev. B: Condens. Matter **55**, 8067 (1997).
13. R. Laiho, K. G. Lisunov, E. Lähderanta, M. A. Shakhov, V. N. Stamov, V. S. Zakhvalinskii, V. L. Kozhevnikov, I. A. Leonidov, E. B. Mitberg, and M. V. Patrakeev, J. Phys.: Condens. Matter **17**, 3429 (2005).
14. R. Laiho, K. G. Lisunov, E. Lähderanta, V. N. Stamov, V. S. Zakhvalinskii, Ph. Colomban, P. A. Petrenko, and Yu. P. Stepanov, J. Phys.: Condens. Matter **17**, 105 (2005).
15. A. S. Alexandrov and A. M. Bratkovsky, J. Appl. Phys. **87**, 5016 (2000).
16. T. G. Castner, in *Hopping Transport in Solids*, Ed. by M. Pollak and B. Shklovskii (Elsevier, Amsterdam, 1991), p. 3.
17. N. F. Mott, *Metal–Insulator Transitions* (Taylor and Francis, London, 1990).
18. *Colossal Magnetoresistance of Oxides*, Ed. by Y. Tokura (Gordon and Breach, Amsterdam, 2000).
19. V. Laukhil, J. Fontcuberta, J. L. Garcia-Munoz, and X. Obradors, Phys. Rev. B: Condens. Matter **56**, 10009 (1997).
20. V. Moshnyaga, S. Klimm, E. Gommert, R. Tidecks, S. Horn, and K. Samwer, J. Appl. Phys. **88**, 5305 (2000).

Translated by G. Skrebtsov

Copyright of Physics of the Solid State is the property of Springer Science & Business Media B.V. and its content may not be copied or emailed to multiple sites or posted to a listserv without the copyright holder's express written permission. However, users may print, download, or email articles for individual use.